

This discussion paper is/has been under review for the journal Atmospheric Chemistry and Physics (ACP). Please refer to the corresponding final paper in ACP if available.

# Estimation of aerosol water and chemical composition from AERONET at Cabauw, the Netherlands

A. J. van Beelen<sup>1</sup>, G. J. H. Roelofs<sup>1</sup>, O. P. Hasekamp<sup>2</sup>, J. S. Henzing<sup>3</sup>, and T. Röckmann<sup>1</sup>

<sup>1</sup>Institute for Marine and Atmospheric research Utrecht (IMAU), P.O. Box 80005, Utrecht University, Utrecht, the Netherlands

<sup>2</sup>Netherlands Institute for Space Research (SRON), Sorbonnelaan 2, 3584 CA Utrecht, the Netherlands

<sup>3</sup>Netherlands Organisation for Applied Scientific Research, TNO, P.O. Box 80015, Utrecht, the Netherlands

Received: 26 March 2013 – Accepted: 9 May 2013 – Published: 10 June 2013

Correspondence to: A. J. van Beelen (a.j.vanbeelen@uu.nl)

Published by Copernicus Publications on behalf of the European Geosciences Union.

ACPD

13, 15191–15232, 2013

Estimation of aerosol composition from AERONET

A. J. van Beelen et al.

Title Page

Abstract

Introduction

Conclusions

References

Tables

Figures

◀

▶

◀

▶

Back

Close

Full Screen / Esc

Printer-friendly Version

Interactive Discussion



## Abstract

Remote sensing of aerosols provides important information on the atmospheric aerosol abundance. However, due to the hygroscopic nature of aerosol particles observed aerosol optical properties are influenced by atmospheric humidity, and the measurements do not unambiguously characterize the aerosol dry mass and composition which complicates the comparison with aerosol models. In this study we derive aerosol water and chemical composition by a modeling approach that combines individual measurements of remotely sensed aerosol properties (e.g. optical thickness, single scattering albedo, refractive index and size distribution) from an AERONET (Aerosol Robotic Network) sun-photometer with radiosonde measurements of relative humidity. The model simulates water uptake by aerosols based on the chemical composition and size distribution. A minimization method is used to calculate aerosol composition and concentration, which are then compared to in situ measurements from the Intensive Measurement Campaign At the Cabauw Tower (IMPACT, May 2008, the Netherlands). Computed concentrations show reasonable agreement with surface observations and follow the day-to-day variability in observations. Total dry mass ( $33 \pm 12 \mu\text{g m}^{-3}$ ) and black carbon concentrations ( $0.7 \pm 0.3 \mu\text{g m}^{-3}$ ) are generally accurately computed. The uncertainty in the AERONET (real) refractive index (0.025–0.05) introduces larger uncertainty in the modeled aerosol composition (e.g. sulfates, ammonium nitrate or organic matter) and leads to an uncertainty of 0.1–0.25 in aerosol water volume fraction. Water volume fraction is highly variable depending on composition, up to >0.5 at 70–80 % and <0.1 at 40 % relative humidity.

## 1 Introduction

Atmospheric aerosol particles interact directly and indirectly, i.e., through cloud albedo and lifetime, with radiation (Lohmann and Feichter, 2005). Aerosols influence weather and climate through visibility, sunshine duration, global radiation and temperature, as

ACPD

13, 15191–15232, 2013

## Estimation of aerosol composition from AERONET

A. J. van Beelen et al.

[Title Page](#)

[Abstract](#)

[Introduction](#)

[Conclusions](#)

[References](#)

[Tables](#)

[Figures](#)

◀

▶

◀

▶

[Back](#)

[Close](#)

[Full Screen / Esc](#)

[Printer-friendly Version](#)

[Interactive Discussion](#)



Title Page

Abstract

Introduction

Conclusions

References

Tables

Figures

◀

▶

◀

▶

Back

Close

Full Screen / Esc

Printer-friendly Version

Interactive Discussion



has been observed on regional (e.g. Van Beelen and Van Delden, 2012) and global scales (Wang et al., 2009; Wild et al., 2007; Forster et al., 2007). Relatively large uncertainties are associated with the aerosol radiative forcing. Estimates of radiative forcing from models range from  $-0.2$  to  $-0.9 \text{ W m}^{-2}$  for the direct effect and  $-0.5$  and  $-1.5 \text{ W m}^{-2}$  for the indirect effect (Forster et al., 2007; Quaas et al., 2009) while remote sensing estimates yield between  $-0.9$  and  $-1.9 \text{ W m}^{-2}$  for the direct effect (Bellouin et al., 2005; Quaas et al., 2008) and  $-0.2 \pm 0.1 \text{ W m}^{-2}$  for the indirect effect (Quaas et al., 2008). The uncertainty in aerosol forcing leads to large uncertainties in estimates of climate sensitivity and future projections of climate change (Andreae et al., 2005).

A better characterization of the aerosol chemical composition and hygroscopicity is a necessary step in narrowing down these uncertainties. Aerosol properties such as size distribution and chemical composition are often measured in situ, for example during dedicated measurement campaigns (e.g. Yu et al., 2009; Kulmala et al., 2011). These measurements are relatively detailed and accurate but they are only representative for small areas, most of which are in the Northern Hemisphere. Satellite remote sensing, on the other hand, provides daily measurements of aerosol optical properties (e.g., aerosol optical thickness, refractive index) and aerosol size that cover the whole globe. However, remotely sensed aerosol optical thickness (AOT) also reflects a contribution of aerosol water. The amount of aerosol water, and thus total aerosol mass and size, depends strongly on the hygroscopicity of the aerosol species and relative humidity (RH), which hampers validation of aerosol properties in aerosol-climate models.

In order to quantify the water contribution to AOT, several studies have retrieved aerosol wet growth or scattering enhancement factors due to aerosol water uptake. Schuster et al. (2009) derive the aerosol water fraction directly from measurements of the refractive index and mass conservation, but they apply an empirical relation to constrain the insoluble to soluble aerosol mass ratio. Jeong et al. (2007) derive vertical profiles of the aerosol humidification factor (the ratio of scattering of aerosol at ambient RH and at dry (low RH) conditions) over the Southern Great Plains (USA) using airborne aerosol measurements of scattering and absorption under high and

Estimation of aerosol composition from AERONET

A. J. van Beelen et al.

[Title Page](#)

[Abstract](#)

[Introduction](#)

[Conclusions](#)

[References](#)

[Tables](#)

[Figures](#)

[◀](#)

[▶](#)

[◀](#)

[▶](#)

[Back](#)

[Close](#)

[Full Screen / Esc](#)

[Printer-friendly Version](#)

[Interactive Discussion](#)



## 2 Methodology

### 2.1 Model

We use a microphysical aerosol model that calculates aerosol water uptake by considering aerosol chemical composition, size distribution and relative humidity. The aerosol optical properties are computed and compared to AERONET retrievals. Aerosol chemical composition and size distribution are found using an optimization method. This involves inverting the following equation:

$$\mathbf{y} = F(\mathbf{x}) + \mathbf{e}_y, \quad (1)$$

Here,  $F$  is our forward model in which aerosol water uptake and optical properties are calculated. The state vector  $\mathbf{x}$  contains the parameters which can be adjusted by the minimization routine. It is initialized with estimates of the mass concentrations of the dry aerosol chemical composition, size distribution and RH, which are then used to calculate aerosol water uptake and optical properties. The measurement vector  $\mathbf{y}$  contains the AERONET retrievals and RH as a prior based on radiosonde measurements.  $\mathbf{e}_y$  denotes the uncertainty estimates of the parameters in  $\mathbf{y}$ . In an iterative procedure the parameters in  $\mathbf{x}$  are adjusted so that the discrepancies between modeled and observed aerosol optical properties, size distribution and RH are minimized. An overview of the model structure is presented in Fig. 1.

#### 2.1.1 Aerosol: initialization, water uptake and optical properties

Table 1 and 2 present an overview of the parameters in  $\mathbf{x}$  and  $\mathbf{y}$  together with their uncertainty estimates used in this study. The model describes aerosol using dry mass mixing ratios, number concentrations and (geometric) standard deviations of lognormal fine and coarse modes, assuming internally mixed spherical particles. Each mode is represented by 100 size bins between droplet radii of 0.005 and 50  $\mu\text{m}$  for accurate description of Mie scattering. Aerosol chemical species considered by the model are

Title Page

Abstract

Introduction

Conclusions

References

Tables

Figures

|◀

▶|

◀

▶|

Back

Close

Full Screen / Esc

Printer-friendly Version

Interactive Discussion



## Estimation of aerosol composition from AERONET

A. J. van Beelen et al.

[Title Page](#)

[Abstract](#)

[Introduction](#)

[Conclusions](#)

[References](#)

[Tables](#)

[Figures](#)

◀

▶

◀

▶

[Back](#)

[Close](#)

[Full Screen / Esc](#)

[Printer-friendly Version](#)

[Interactive Discussion](#)



**Estimation of aerosol composition from AERONET**

A. J. van Beelen et al.

[Title Page](#)[Abstract](#)[Introduction](#)[Conclusions](#)[References](#)[Tables](#)[Figures](#)[◀](#)[▶](#)[◀](#)[▶](#)[Back](#)[Close](#)[Full Screen / Esc](#)[Printer-friendly Version](#)[Interactive Discussion](#)

**Estimation of aerosol composition from AERONET**

A. J. van Beelen et al.

[Title Page](#)[Abstract](#)[Introduction](#)[Conclusions](#)[References](#)[Tables](#)[Figures](#)[◀](#)[▶](#)[Back](#)[Close](#)[Full Screen / Esc](#)[Printer-friendly Version](#)[Interactive Discussion](#)

(RRI) between 1.56 and 1.60 (e.g. Stelson, 1990), which is used in our study (Table 4), but sometimes a much lower RRI of 1.42 is used (e.g. Weast, 1987).

Sea salt and dust have been omitted from this study since only very few measurements were influenced by these species at Cabauw during May 2008. Though Cabauw is located only 50 km from the coast, the neglect of sea salt in the aerosol is a good assumption because the first half of May is dominated by continental air masses; and although surface measurements of  $\text{Na}^+$  are not available,  $\text{Cl}^-$  concentrations are very low ( $\ll 1 \mu\text{g m}^{-3}$ ). Furthermore, we limited the number of parameters in the optimization by taking representative ammonium:sulfate and nitrate:sulfate ratios, based on a scheme from Gysel et al. (2007). The ammonium to sulfate mass ratio which corresponds best to surface measurements is 1.8. Surface observations of ammonium nitrate during May 2008 correlate well ( $R^2 = 0.71$ ) with that of sulfate, the mass ratio of ammonium nitrate to sulfate is 1.3.

### 2.1.2 Minimization procedure

Modeled aerosol optical properties and size distribution are compared to observations from the AERONET optical ground-based aerosol monitoring station located at Cabauw during May 2008. We use the AERONET level 1.5 inversions (Dubovik and King, 2000; cloud screened but not quality assured, Smirnov et al., 2000), because level 2.0 data of SSA and RI were not available during most of May 2008. Parameters used are AOT, SSA and complex refractive index (RRI and IRI) data at 4 wavelengths ( $\lambda = 440, 675, 870$  and  $1020 \text{ nm}$ ), and the volume size distribution ( $V_i$ ), resolved in 22 size bins between 0.05 and  $15 \mu\text{m}$  (Table 2). The model size distribution is rebinned to the AERONET resolution before comparison. The AERONET retrieval assumes that aerosols are homogeneous internally mixed particles with a single wavelength dependent RI, while our model assumes a bi-modal lognormal size distribution with homogeneous composition (and thus a single RI) in each individual mode, because aerosol RI is often size dependent (e.g. Benko et al., 2009).

Title Page	
Abstract	Introduction
Conclusions	References
Tables	Figures
◀	▶
◀	▶
Back	Close
Full Screen / Esc	
Printer-friendly Version	
Interactive Discussion	

AERONET SSA and RI are relatively accurate for  $\text{AOT} > 0.2$  but their inaccuracy is larger for smaller AOT. The uncertainties ( $e_y$ ) used in our model are derived from Dubovik et al. (2000) and can be found in Table 2. The uncertainty in the AERONET volume distribution is 15% between 0.1 and 7  $\mu\text{m}$ , increasing up to 100% at the distribution edges. The column average RH from the sounding is used both as an initial guess ( $x$ ) to calculate aerosol water uptake, as well as a parameter ( $\text{RH}_{\text{prior}}$ , in  $y$ ) which is used in the optimization. It can be adjusted by the model if this leads to a better fit with the AERONET aerosol parameters, but changing RH from its prior value will also contribute to the cost function. The variance of the sounding RH in a layer of 2 km thickness near the ground is used as an uncertainty estimate, and is generally in the order of 0.1 (i.e., 10%).

A cost function  $\phi(x)$  quantifies the total difference between modeled ( $F(x)$ ) and observed ( $y$ ) aerosol parameters:

$$\phi(x) = \sum_{i=1}^N \left( \frac{F(x) - y}{w e_y} \right)^2, \quad (2)$$

The difference between modeled and observed aerosol parameters is weighted by the uncertainties in  $y$  together with a weighting factor  $w$  that considers interdependency of the variables, and then summed over  $N$ , the number of parameters in  $y$ .

The routine searching for the minimum of the cost function is known as “amoeba” (Nelder and Mead, 1965). It uses a simplex based on the logarithm of the model parameters (i.e. mass concentrations of the components in each mode, the number concentration and standard deviation of the lognormal distribution of each mode and the RH, Table 1). Amoeba finds a minimum on nearly all parameter spaces, but convergence does not always result in the absolute minimum. The probability of finding the latter is greatly improved by restarting amoeba on a previously found minimum until the cost function converges.



## 2.2 IMPACT observations

### 2.2.1 AERONET

The optimization procedure uses AERONET retrievals of AOT, RI and aerosol size at Cabauw during the first half of May 2008. This period was characterized by relatively

- 5 fair weather. Later during the month the weather became more unsettled with cloudy and rainy periods (e.g., Roelofs et al., 2010; Hamburger et al., 2011) and only few available AERONET observations. Therefore we focus our analysis on the first half of the month.

AERONET AOT and Ångström exponent during this period are shown in Fig. 2. Between 6 and 12 May, dry continental air was advected from the east. The AOT is generally between 0.2–0.4, and the Ångström exponent is generally well above 1, indicating the absence of a significant coarse mode fraction. During daytime a well-mixed boundary layer was formed between 0 and 2 km altitude above the surface. Figure 2 also shows the RH averaged over the boundary layer as well as the RRI. The atmosphere is relatively dry, with RH between 40 and 60 % except for the first three days, and the variability during a day is on the order of 10–20 %. AOT displays a distinct daily variability with a minimum around noon when RH is generally lowest. On the driest days, May 9 and 10, RH does not have a strong daily variation and the smallest AOT is found in the morning. The RRI measured by AERONET ranges between 1.33 and 1.60. It is highly variable, even during a single day (e.g., 9 and 10 May) and appears to be only weakly correlated with RH.

### 2.2.2 Aerosol chemical composition

Optimized solutions for aerosol composition are validated with measurements from the IMPACT campaign (Kulmala et al., 2011; Mensah et al., 2012), carried out at Cabauw in the Netherlands as part of the European Integrated Project on Aerosol Cloud Climate and Air Quality interactions (EUCAARI, Kulmala et al., 2009, 2011). The Cabauw

[Title Page](#)

[Abstract](#)

[Introduction](#)

[Conclusions](#)

[References](#)

[Tables](#)

[Figures](#)

◀

▶

[Back](#)

[Close](#)

[Full Screen / Esc](#)

[Printer-friendly Version](#)

[Interactive Discussion](#)



**Estimation of aerosol composition from AERONET**

A. J. van Beelen et al.

[Title Page](#)[Abstract](#)[Introduction](#)[Conclusions](#)[References](#)[Tables](#)[Figures](#)[|◀](#)[▶|](#)[◀](#)[▶|](#)[Back](#)[Close](#)[Full Screen / Esc](#)[Printer-friendly Version](#)[Interactive Discussion](#)

Experimental Site for Atmospheric Research (CESAR, Russchenberg et al., 2005; <http://www.cesar-observatory.nl>; 51.97° N, 4.93° E, –0.7 m a.s.l.) is located in a typical rural area in the central Netherlands with nearly flat orography in all directions. This area is also well representative of Central Europe. During IMPACT, aerosol and cloud data were gathered near the 213 m high Cabauw Tower. Balloon sounding, helicopter and aircraft measurements from a wider area around Cabauw are also available.

Surface concentrations of inorganic aerosol species  $\text{NO}_3^-$ ,  $\text{SO}_4^{2-}$ ,  $\text{NH}_4^+$ ,  $\text{Na}^+$  and  $\text{Cl}^-$  were measured with a MARGA instrument (Monitor for Aerosols and Gases, Applikon Analytical BV; ten Brink et al., 2007; Thomas et al., 2009), with an hourly resolution and a measurement error smaller than 10 % (Schaap et al., 2011 and references therein). Aerosol organic concentrations were measured with an Aerodyne Aerosol Mass Spectrometer (HR-ToF-AMS) (Jülich ICG-2, Canagaratna et al., 2007), with a 5 min time resolution from an inlet at 60 m altitude (Mensah et al., 2012). Black carbon mass concentrations are measured with a Multi-Angle Absorption Photometer (TNO, MAAP Thermo Scientific Model 5012; Petzold et al., 2005) with a resolution of 5 min and uncertainty of 12 % (Petzold and Schönlinner, 2004).

We note that measured organic masses are effectively  $\text{PM}_1$  (100 % transmission in range 70–500 nm and 50 % for particles with 1  $\mu\text{m}$  diameter). To compare these with the optimized organic mass, which is essentially  $\text{PM}_{10}$ , we scaled the AMS measurements to  $\text{PM}_{10}$  based on the observed sulfate masses from MARGA and the AMS. This implies that sulfate and organics are distributed similarly over aerosol size, which is a reasonable assumption because a significant fraction of secondary organic as well as inorganic (sulfate) aerosol matter formed in the gas phase deposits onto the fine mode (Kulmala et al., 2004; Kanakidou et al., 2005; Hallquist et al., 2009).

### 3 Results

The refractive index is a crucial parameter in the optimization of the aerosol chemical composition. Figure 3 shows a comparison between the optimized RRI and the

**Estimation of aerosol composition from AERONET**

A. J. van Beelen et al.

[Title Page](#)[Abstract](#)[Introduction](#)[Conclusions](#)[References](#)[Tables](#)[Figures](#)[◀](#)[▶](#)[◀](#)[▶](#)[Back](#)[Close](#)[Full Screen / Esc](#)[Printer-friendly Version](#)[Interactive Discussion](#)

Title Page

Abstract

Introduction

Conclusions

References

Tables

Figures

◀

▶

◀

▶

Back

Close

Full Screen / Esc

Printer-friendly Version

Interactive Discussion



values and associated standard deviation are significantly larger ( $38.5 \pm 25.2 \mu\text{g m}^{-3}$ ) than observed. Note however that this is predominately caused by a few outliers, the modeled and observed medians are still reasonably close (31.5 versus  $28.7 \mu\text{g m}^{-3}$ ).

Although the daily averages of computed results and the observations are in close agreement during this period, the daily cycle of the computed aerosol mass is opposite to that of the observations, with the former showing an increase and the latter a decrease during the day. This is partly due to the different ways that boundary layer meteorology influences columnar mass as compared to surface concentration. During the early morning hours, aerosols are trapped in a thin stable layer near the surface. This layer will rapidly mix with the atmosphere above when heated by the sun, leading to a reduction in the aerosol concentration near the surface without changing the total column aerosol burden. Additionally, rapidly rising temperatures near the surface during the day shifts the partitioning of semi-volatile gases such as ammonium nitrate and volatile organic compounds to the gas phase (Schaap et al., 2011; Aan de Brugh et al., 2012). More abundant road traffic and photochemical production of secondary aerosol during daytime may be the reason why the computed (column average) dry mass increases in the afternoon.

The total dry mass is based on the optimized mass concentrations of the individual aerosol species. Table 6 lists modeled (total column average) and observed (surface) mass concentrations. The agreement between both is reasonable, i.e., within the computed standard deviations, with computed BC and OC somewhat smaller, and sulfate, nitrate and ammonium larger than observed.

This is further illustrated in Fig. 5, showing computed and observed black carbon, and Fig. 6, showing comparisons for the inorganic salt ions ( $\text{SO}_4^{2-}$ ,  $\text{NH}_4^+$  and  $\text{NO}_3^-$ ) and organic matter. Optimized BC concentrations (Fig. 5) fall within the same range as observed concentrations. On some days the observed hourly variability, represented by the red line, appears to be captured by the model (5, 6, 13 May). A significant overestimation occurs on 4 May when traces of Sahara dust were present over the Cabauw region (Roelofs et al., 2010). Since mineral dust is neglected in this study, the

<a href="#">Title Page</a>	
<a href="#">Abstract</a>	<a href="#">Introduction</a>
<a href="#">Conclusions</a>	<a href="#">References</a>
<a href="#">Tables</a>	<a href="#">Figures</a>
<a href="#"></a>	<a href="#"></a>
<a href="#"></a>	<a href="#"></a>
<a href="#">Back</a>	<a href="#">Close</a>
<a href="#">Full Screen / Esc</a>	
<a href="#">Printer-friendly Version</a>	
<a href="#">Interactive Discussion</a>	



associated scattering and absorption is now attributed to the other compounds in our model. Nevertheless, we conclude that the optimization performs relatively well for BC, especially considering the uncertainties in AERONET SSA and IRI.

Figure 6 shows that optimized concentrations generally follow the day-to-day variability of the observed concentrations, especially for sulfate, ammonium and nitrate. Concentrations are relatively low on 1–2 May, 5–7 May and 11–12 May, while higher concentrations are observed and modeled between May 7–10 and May 13–14. We note that on May 11–12 a brief period with north-easterly and relatively clean winds occurred, characterized by a small AOT (0.1–0.2), low RH and high refractive index (RRI > 1.48; Fig. 2). Our model calculates concentrations of nitrate and ammonium that are considerably smaller than those of the surrounding days, in good agreement with the observations.

The largest discrepancies are found on 7–9 May and later on 14 May, when our method overestimates concentrations of sulfate and ammonia but underestimates OC. This relates to days when the RI shows strong hourly variability even though RH is relatively constant. For relatively high RRI (> 1.52) our method calculates relatively high concentrations of OC whereas for relatively small RRI (< 1.44) water and inorganic salts dominate the modeled aerosol composition. We note that the RRI of the mixture of inorganic salts is only slightly lower than that of OC (approx. 1.53, Table 4) while the assumed hygroscopicity of OC is much smaller than that of inorganic salts. As a result our model computes a predominantly organic composition at relatively high RRI also at high RH.

The resulting aerosol water fraction is displayed in Fig. 7. At high RH (e.g. 70–80 %) approximately half of the total aerosol volume, and therefore nearly half of the optical thickness, consists of water. At low RH (e.g. 40 %) the aerosol water fraction decreases to less than 0.1. Note the strong variability of the aerosol water fraction on 7–9 May, associated with the variability in AERONET RRI during each day.

The results are summarized in Fig. 8, which shows the computed volume fractions of the aerosol inorganic species, OC, BC and water, as function of model optimized RRI.

Inorganic and organic fractions depend strongly on RRI between 1.40–1.55, with decreasing inorganic and water volume fractions and increasing organic fractions for high RRI. Discrepancies from this behavior (e.g. at RRI = 1.41 in Fig. 8) are associated with the effects of water uptake from ambient RH: at very high relative humidity the aerosol 5 can still contain a significant fraction of organics at a relatively low RRI, while this is not possible at somewhat lower RH. The optimization of aerosol chemical composition is therefore highly sensitive to RI, and to errors in the AERONET inversions of RI, the description of aerosol RI as a complex mixture of components and the optical model of scattering and absorption. The uncertainty in AERONET RRI (i.e. 0.025–0.05) will 10 lead to 10–25 % (absolute) difference in water volume fraction for RRI between 1.40 and 1.50.

## 4 Conclusions and discussion

We have presented an optimization technique that derives aerosol chemical composition from remotely sensed aerosol optical thickness, refractive index, size distribution 15 and measurements of relative humidity. The model calculates aerosol water uptake and optical properties of a mixture of sulfate, ammonium, nitrate, black carbon and organic matter, assuming a single homogeneous layer of air, aerosol and RH. Aerosol composition and concentration are determined by minimizing the difference between modeled and AERONET aerosol properties and effective RH. The method is applied to individual 20 measurements so that short-term variability of the concentrations is resolved. This enables study and aerosol-climate model validation of the effects of temporal variations in e.g., photochemistry, humidity and emissions on the aerosol concentration and chemical composition (Derksen et al., 2011; Aan de Brugh et al., 2012). The technique is validated against surface concentrations observed during the IMPACT measurement campaign that was carried out at Cabauw (the Netherlands, May 2008).

On most days the optimized column dry mass concentration is reasonably close to the surface observations from MARGA and the Jülich ICG-2 aerosol mass spectrom-

<a href="#">Title Page</a>	
<a href="#">Abstract</a>	<a href="#">Introduction</a>
<a href="#">Conclusions</a>	<a href="#">References</a>
<a href="#">Tables</a>	<a href="#">Figures</a>
<a href="#">◀</a>	<a href="#">▶</a>
<a href="#">◀</a>	<a href="#">▶</a>
<a href="#">Back</a>	<a href="#">Close</a>
<a href="#">Full Screen / Esc</a>	
<a href="#">Printer-friendly Version</a>	
<a href="#">Interactive Discussion</a>	



eter, especially during a series of dry and sunny days between 6 and 12 May. During this time most water vapor and aerosols were confined to a boundary layer of approximately 2 km deep, consistent with our assumptions. For the individual aerosol species sulfate, nitrate, ammonium, BC and OC the resulting concentrations compare relatively well with observations and reflect realistic day-to-day variability.

Nevertheless, discrepancies occur for several reasons.

1. We assume that aerosol mass and RH are distributed uniformly over a 2 km layer. Therefore, our optimization results reflect columnar aerosol properties, while observations (e.g. MARGA, AMS) reflect surface concentrations. This especially hampers a good representation of the daily cycle of aerosol concentration at the surface since the daily cycle in the boundary layer height is not considered. Also, averaging RH in the boundary layer leads to an underestimation of aerosol water uptake due to the nonlinear dependence of aerosol water uptake on RH (e.g., Yeong et al., 2007; Bian et al., 2009; Zieger et al., 2011). Finally, RH and the concentration and chemical composition vary with altitude, which introduces inaccuracy in modeled column and surface concentrations. An important process in this respect is the strong temperature and humidity dependence of the gas-particle partitioning of ammonium nitrate, leading to an increase of aerosol mass with altitude (Morgan et al., 2010; Aan de Brugh et al., 2012). Such discrepancies may be reduced in future studies by including also vertical information from observed aerosol extinction profiles, e.g., from lidar, and by consideration of different aerosol layers during optimization.
2. The most important parameter in the optimization of the aerosol chemical composition is the RRI, and results indicate that this parameter alone to large extent already reflects relative amounts of aerosol hydrophilic inorganic matter, relatively hydrophobic organic matter, and aerosol water. Uncertainties in our optimization results are primarily associated with the uncertainties of RI of particular components. The RI of aerosol components such as ammonium nitrate, OC, BC and

<a href="#">Title Page</a>	
<a href="#">Abstract</a>	<a href="#">Introduction</a>
<a href="#">Conclusions</a>	<a href="#">References</a>
<a href="#">Tables</a>	<a href="#">Figures</a>
<a href="#">◀</a>	<a href="#">▶</a>
<a href="#">◀</a>	<a href="#">▶</a>
<a href="#">Back</a>	<a href="#">Close</a>
<a href="#">Full Screen / Esc</a>	
<a href="#">Printer-friendly Version</a>	
<a href="#">Interactive Discussion</a>	



<a href="#">Title Page</a>	
<a href="#">Abstract</a>	<a href="#">Introduction</a>
<a href="#">Conclusions</a>	<a href="#">References</a>
<a href="#">Tables</a>	<a href="#">Figures</a>
<a href="#">◀</a>	<a href="#">▶</a>
<a href="#">◀</a>	<a href="#">▶</a>
<a href="#">Back</a>	<a href="#">Close</a>
<a href="#">Full Screen / Esc</a>	
<a href="#">Printer-friendly Version</a>	
<a href="#">Interactive Discussion</a>	

dust, strongly depends on the actual chemical composition or particulate state. Changing model RI within the uncertainty ranges affects the results: using a higher RI for OC, i.e. RRI = 1.60 instead of 1.56, together with a smaller RRI for ammonium nitrate (1.42 instead of 1.56) improves the overall agreement with AERONET, the RH and observed surface concentrations, especially for OC. It is not clear though that such changes are justified, especially for ammonium nitrate. Furthermore, sensitivity studies suggest that the modeled dry mass and water are not very sensitive to the choice of the dry RI or the mixing rule used to determine the RI for a mixture of components, because the effect of water uptake on the RI is much larger.

- 5
- 10
- 15
- 20
- 25
3. Uncertainties in the observed RI affect the modeled aerosol composition considerably. For example, for RRI between 1.40 and 1.50 the uncertainty in AERONET RRI (i.e. 0.025–0.05) will lead to 10–25 % (absolute) difference in water volume fraction. AERONET RRI shows very large variations, also during the course of a single day. The correlation between radiosonde effective RH and the AERONET RRI is low ( $R^2 \sim 0.16$ ). This suggests unrealistic variations in aerosol composition and hygroscopicity during a day, considering the stable and fair weather conditions in the period under research. Another, minor, inaccuracy is associated with the wavelength dependence of the AERONET RRI. For most compounds, especially OC, RI decreases with wavelength (Table 4), but AERONET RI is highly variable and on several occasions increases with wavelength, leading to discrepancies between modeled and observed aerosol optical properties, especially at 440 nm. This impedes our ability to distinguish black carbon from absorbing organic matter (“brown carbon”) (e.g. Bergstrom et al., 2007; Russell et al., 2010; Arola et al., 2011) because the IRI strongly increases towards the ultra violet wavelengths for OC, contrary to that of BC (Jacobson, 1999; Kirchstetter et al., 2004; Sun et al., 2007; and Chen and Bond, 2010).

Title Page

Abstract

Introduction

Conclusions

References

Tables

Figures

◀

▶

Back

Close

Full Screen / Esc

Printer-friendly Version

Interactive Discussion



Our technique may be extended to global scales by using satellite remote sensing of aerosol properties (e.g. from the Polarization and Directionality of Earth Reflectances (POLDER) instrument onboard the PARASOL satellite (e.g. Hasekamp et al., 2011; Tanré et al., 2011). Accurate retrieval of the refractive index is vital for determination of column aerosol composition; in light of this the loss of the Aerosol Polarimetry Sensor (APS) with the Glory satellite is extremely unfortunate.

*Acknowledgements.* We thank AERONET and Gerrit de Leeuw for their effort in establishing and maintaining the Cabauw site. We also thank the researchers conducting the measurements during the IMPACT 2008 campaign, made possible through financial support of the Sixth Framework European Integrated project on Aerosol Cloud Climate and Air Quality Interactions (EUCAARI), specifically to Harry ten Brink and René Otjes (ECN) for providing the MARGA data; Th. F. Mentel and A. Kiendler-Scharr (Forschungszentrum Jülich GmbH, Germany) for the ICG-2 AMS data; Richard Rothe (KNMI) for the radiosonde data; Dave Donovan (KNMI) for the UV lidar data and Arnoud Apituley (RIVM) for the CAELI data. We acknowledge the project and support of the European Community – Research Infrastructure Action under the FP7 “Capacities” specific program for Integrating Activities, ACTRIS Grant Agreement no. 262254.

## References

- Aan de Brugh, J. M. J., Henzing, J. S., Schaap, M., Morgan, W. T., van Heerwaarden, C. C., Weijers, E. P., Coe, H., and Krol, M. C.: Modelling the partitioning of ammonium nitrate in the convective boundary layer, *Atmos. Chem. Phys.*, 12, 3005–3023, doi:10.5194/acp-12-3005-2012, 2012.
- Andreae, M. O., Jones, C. D., and Cox, P. M.: Strong present day cooling implies a hot future, *Nature*, 435, 1187–1190, doi:10.1038/nature03671, 2005.
- Apituley, A., Wilson, K. M., Potma, C., Volten, H., and de Graaf, M.: Performance Assessment and Application of Caeli – A high performance Raman lidar for diurnal profiling of Water Vapour, Aerosols and Clouds, *Proceedings of the 8th International Symposium on Tropospheric Profiling*, 19–23 October 2009, Delft, the Netherlands, 2009.

Arola, A., Schuster, G., Myhre, G., Kazadzis, S., Dey, S., and Tripathi, S. N.: Inferring absorbing organic carbon content from AERONET data, *Atmos. Chem. Phys.*, 11, 215–225, doi:10.5194/acp-11-215-2011, 2011.

Bellouin, N., Boucher, O., Haywood, J., and Reddy, M. S.: Global estimate of aerosol direct radiative forcing from satellite measurements, *Nature*, 438, 1138–1141, doi:10.1038/nature04348, 2005.

Benko, D., Molnár, A., and Imre, K.: Study on the size dependence of complex refractive index of atmospheric aerosol particles over Central Europe, *Időjárás*, 113, 157–175, 2009.

Bergstrom, R. W., Pilewskie, P., Russell, P. B., Redemann, J., Bond, T. C., Quinn, P. K., and Sierau, B.: Spectral absorption properties of atmospheric aerosols, *Atmos. Chem. Phys.*, 7, 5937–5943, doi:10.5194/acp-7-5937-2007, 2007.

Bian, H., Chin, M., Rodriguez, J. M., Yu, H., Penner, J. E., and Strahan, S.: Sensitivity of aerosol optical thickness and aerosol direct radiative effect to relative humidity, *Atmos. Chem. Phys.*, 9, 2375–2386, doi:10.5194/acp-9-2375-2009, 2009.

Bohren, C. F. and Huffman, D. R.: *Absorption and scattering of light by small particles*, Wiley Professional Paperback Series, Wiley-Interscience, New York, USA, 1998.

Bond, T. C. and Bergstrom, R. W.: Light absorption by carbonaceous particles: An investigative review, *Aerosol Sci. Technol.*, 40, 27–67, doi:10.1080/02786820500421521, 2006.

Canagaratna, M. R., Jayne, J. T., Jimenez, J. L., Allan, J. D., Alfarra, M. R., Zhang, Q., Onasch, T. B., Drewnick, F., Coe, H., Middlebrook, A., Delia, A., Williams, L. R., Trimborn, A. M., Northway, M. J., DeCarlo, P. F., Kolb, C. E., Davidovits, P., and Worsnop, D. R.: Chemical and microphysical characterization of ambient aerosols with the aerodyne aerosol mass spectrometer, *Mass Spectrom. Rev.*, 26, 185–222, doi:10.1002/mas.20115, 2007.

Chang, H. and Charalampopoulos, T. T.: Determination of the wavelength dependence of refractive indices of flame soot, *Proc. R. Soc. London, Ser. A*, 430, 577–591, 1990.

Chen, Y. and Bond, T. C.: Light absorption by organic carbon from wood combustion, *Atmos. Chem. Phys.*, 10, 1773–1787, doi:10.5194/acp-10-1773-2010, 2010.

Derkzen, J. W. B., Roelofs, G. J., Otjes, R., de Leeuw, G., and Röckmann, T.: Impact of ammonium nitrate chemistry on the AOT in Cabauw, the Netherlands, *Atmos. Environ.*, 45, 5640–5646, doi:10.1016/j.atmosenv.2011.02.052, 2011.

Dick, W. D., Saxena, P., and McMurry, H. P.: Estimation of water uptake by organic compounds in submicron aerosols measured during the Southeastern Aerosol and Visibility Study, *J. Geophys. Res.*, 105, 1471–1479, doi:10.1029/1999JD901001, 2000.

[Title Page](#)[Abstract](#)[Introduction](#)[Conclusions](#)[References](#)[Tables](#)[Figures](#)[◀](#)[▶](#)[◀](#)[▶](#)[Back](#)[Close](#)[Full Screen / Esc](#)[Printer-friendly Version](#)[Interactive Discussion](#)

Estimation of aerosol composition from AERONET

A. J. van Beelen et al.

Title Page

Abstract

Introduction

Conclusions

References

Tables

Figures

◀

▶

Back

Close

Full Screen / Esc

Printer-friendly Version

Interactive Discussion



Dinar, E., Mentel, T. F., and Rudich, Y.: The density of humic acids and humic like substances (HULIS) from fresh and aged wood burning and pollution aerosol particles, *Atmos. Chem. Phys.*, 6, 5213–5224, doi:10.5194/acp-6-5213-2006, 2006.

Dinar, E., Riziq, A. A., Spindler, C., Erlick, C., Kiss, G., and Rudich, Y.: The complex refractive index of atmospheric and model humic-like substances (HULIS) retrieved by a cavity ring down aerosol spectrometer (CRD-AS), *Faraday Discuss.*, 137, 279–295, 2008.

Dubovik, O. and King, M. D.: A flexible inversion algorithm for retrieval of aerosol optical properties from Sun and sky radiance measurements, *J. Geophys. Res.*, 105, 20673–20696, 2000.

Dubovik, O., Smirnov, A., Holben, B. N., King, M. D., Kaufman, Y. J., Eck, T. F., and Slutsker, I.: Accuracy assessments of aerosol optical properties retrieved from AERONET sun and sky-radiance measurements, *J. Geophys. Res.*, 105, 9791–9806, 2000.

Erlick, C.: Effective refractive indices of water and sulfate drops containing absorbing inclusions, *J. Atmos. Sci.*, 63, 754–763, 2006.

Erlick, C., Abbatt, J. P., and Rudich, Y.: How Different Calculations of the Refractive Index Affect Estimates of the Radiative Forcing Efficiency of Ammonium Sulfate Aerosols, *J. Atmos. Sci.*, 68, 1845–1852, 2011.

Feingold, G.: Modeling of the first indirect effect: Analysis of measurement requirements, *J. Geophys. Res.*, 30, 1997, doi:10.1029/2003GL017967, 2003.

Forster, P., Ramaswamy, V., Artaxo, P., Berntsen, T., Betts, R., Fahey, D. W., Haywood, J., Lean, J., Lowe, D. C., Myhre, G., Nganga, J., Prinn, R., Raga, G., Schulz, M., and van Dorland, R.: Changes in Atmospheric Constituents and in Radiative Forcing. In: *Climate Change 2007: The Physical Science Basis. Contribution of WGI to the Fourth Assessment Report of the Intergovernmental Panel on Climate Change*, edited by: Solomon, S., Qin, D., Manning, M., Chen, Z., Marquis, M., Averyt, K. B., Tignor, M., and Miller, H. L., Cambridge University Press, Cambridge, UK and New York, NY, USA, 2007.

Ganguly, D., Ginoux, P., Ramaswamy, V., Dubovik, O., Welton, J., Reid, E. A., and Holben, B. N.: Inferring the composition and concentration of aerosols by combining AERONET and MPLNET data: Comparison with other measurements and utilization to evaluate GCM output, *J. Geophys. Res.*, 114, D16203, doi:10.1029/2009JD011895, 2009.

Gysel, M., Crosier, J., Topping, D. O., Whitehead, J. D., Bower, K. N., Cubison, M. J., Williams, P. I., Flynn, M. J., McFiggans, G. B., and Coe, H.: Closure study between chemical composition

**Estimation of aerosol composition from AERONET**

A. J. van Beelen et al.

[Title Page](#)[Abstract](#)[Introduction](#)[Conclusions](#)[References](#)[Tables](#)[Figures](#)[◀](#)[▶](#)[◀](#)[▶](#)[Back](#)[Close](#)[Full Screen / Esc](#)[Printer-friendly Version](#)[Interactive Discussion](#)

- and hygroscopic growth of aerosol particles during TORCH2, *Atmos. Chem. Phys.*, 7, 6131–6144, doi:10.5194/acp-7-6131-2007, 2007.
- Hallquist, M., Wenger, J. C., Baltensperger, U., Rudich, Y., Simpson, D., Claeys, M., Dommen, J., Donahue, N. M., George, C., Goldstein, A. H., Hamilton, J. F., Herrmann, H., Hoffmann, T., Iinuma, Y., Jang, M., Jenkin, M. E., Jimenez, J. L., Kiendler-Scharr, A., Maenhaut, W., McFiggans, G., Mentel, Th. F., Monod, A., Prévôt, A. S. H., Seinfeld, J. H., Surratt, J. D., Szmigielski, R., and Wildt, J.: The formation, properties and impact of secondary organic aerosol: current and emerging issues, *Atmos. Chem. Phys.*, 9, 5155–5236, doi:10.5194/acp-9-5155-2009, 2009.
- Hamburger, T., McMeeking, G., Minikin, A., Birmili, W., Dall’Osto, M., O’Dowd, C., Flentje, H., Henzing, B., Junninen, H., Kristensson, A., de Leeuw, G., Stohl, A., Burkhardt, J. F., Coe, H., Krejci, R., and Petzold, A.: Overview of the synoptic and pollution situation over Europe during the EUCAARI-LONGREX field campaign, *Atmos. Chem. Phys.*, 11, 1065–1082, doi:10.5194/acp-11-1065-2011, 2011.
- Hasekamp, O. P., Litvinov, P., and Butz, A.: Aerosol properties over the ocean from PARASOL multiangle photopolarimetric measurements, *J. Geophys. Res.*, 116, D14204, doi:10.1029/2010JD015469, 2011.
- Hess, M., Koepke, P., and Schult, I.: Optical Properties of Aerosols and Clouds: The Software Package OPAC, *B. Am. Meteorol. Soc.*, 79, 831–844, doi:10.1175/1520-0477(1998)079<0831:OPOAAC>2.0.CO;2, 1998.
- Hoffer, A., Gelencsér, A., Guyon, P., Kiss, G., Schmid, O., Frank, G. P., Artaxo, P., and Andreae, M. O.: Optical properties of humic-like substances (HULIS) in biomass-burning aerosols, *Atmos. Chem. Phys.*, 6, 3563–3570, doi:10.5194/acp-6-3563-2006, 2006.
- Holben, B. N., Eck, T. F., Slutsker, I., Tanre, D., Buis, J. P., Setzer, A., Vermote, E., Reagan, J. A., Kaufman, Y. F., Nakajima, T., Lavenu, F., Jankowiak, I., and Smirnov, A.: AERONET – A Federated Instrument Network and Data Archive for Aerosol Characterisation, *Remote Sens. Environ.*, 66, 1–16, 1998.
- Horvath, H.: Influence of atmospheric aerosols upon the global radiation balance, In Atmospheric Particles IUPAC Series on Analytical and Physical Chemistry of Environmental Systems, John Wiley, New York, Vol. 5, 543–596, 1998.
- Jacobson, M. Z.: Isolating nitrated and aromatic aerosols and nitrated aromatic gases as sources of ultraviolet light absorption, *J. Geophys. Res.*, 104, 3527–3542, 1999.
- Janzen, J.: The refractive index of colloidal carbon, *J. Colloid Interface Sci.*, 69, 436–447, 1979.

Estimation of aerosol composition from AERONET

A. J. van Beelen et al.

Title Page

Abstract

Introduction

Conclusions

References

Tables

Figures

◀

▶

Back

Close

Full Screen / Esc

Printer-friendly Version

Interactive Discussion



Jeong, M. J., Li, Z., Andrews, E., and Tsay, S.-C.: Effect of aerosol humidification on the column aerosol optical thickness over the Atmospheric Radiation Measurement Southern Great Plains site, *J. Geophys. Res.*, 112, D10202, doi:10.1029/2006JD007176, 2007.

Kanakidou, M., Seinfeld, J. H., Pandis, S. N., Barnes, I., Dentener, F. J., Facchini, M. C., Van Dingenen, R., Ervens, B., Nenes, A., Nielsen, C. J., Swietlicki, E., Putaud, J. P., Balkanski, Y., Fuzzi, S., Horth, J., Moortgat, G. K., Winterhalter, R., Myhre, C. E. L., Tsigaridis, K., Vignati, E., Stephanou, E. G., and Wilson, J.: Organic aerosol and global climate modelling: a review, *Atmos. Chem. Phys.*, 5, 1053–1123, doi:10.5194/acp-5-1053-2005, 2005.

Kandler, K., Lieke, K., Benker, N., Emmel, C., Küpper, M., Müller- Ebert, D., Ebert, M., Scheuvens, D., Schladitz, A., Schütz, L., and Weinbruch, S.: Electron microscopy of particles collected at Praia, Cape Verde, during the Saharan Mineral Dust Experiment: particle chemistry, shape, mixing state and complex refractive index, *Tellus B*, 63, 475–496, 2011.

Kinne, S., Lohmann, U., Feichter, J., Timmreck, C., Schulz, M., Ghan, S., Easter, R., Chin, M., Ginoux, P., Takemura, T., Tegen, I., Koch, D., Herzog, M., Penner, J., Pitari, G., Holben, B., Eck, T., Smirnov, A., Dubovik, O., Slutsker, I., Tanré, D., Torres, O., Mishchenko, M., Geogdzhayev, I., Chu, D. A., and Kaufman, Y.: Monthly Averages of Aerosol Properties: A Global comparison among models, satellite data and AERONET ground data, *J. Geophys. Res.*, 108, 4634, doi:10.1029/2001JD001253, 2003.

Kirchstetter, T. W., Novakov, T., and Hobbs, P. V.: Evidence that the spectral dependence of light absorption by aerosols is affected by organic carbon, *J. Geophys. Res.*, 109, D21208, doi:10.1029/2004JD004999, 2004.

Köhler, H.: The nucleus in the growth of hygroscopic droplets, *Trans. Faraday Soc.*, 32, 1152–1161, 1936.

Köpke, P., Hess, M., Schult, I., and Shettle, E. P.: Global Aerosol Data Set, Report No. 243, ISSN: 0937-1060, Max-Planck-Institut für Meteorologie, Hamburg, 1997.

Koren, I., Remer, L., Kaufman, Y. J., Rudich, Y., and Martins, J.: On the twilight zone between clouds and aerosols, *Geophys. Res. Lett.*, 34, L08805, doi:10.1029/2007GL029253, 2007.

Kulmala, M., Kerminen, V. M., Anttila, T., Laaksonen, A., and O'Dowd, C. D.: Organic aerosol formation via sulphate cluster activation, *J. Geophys. Res.*, 109, D04205, doi:10.1029/2003JD003961, 2004.

Kulmala, M., Asmi, A., Lappalainen, H. K., Carslaw, K. S., Pöschl, U., Baltensperger, U., Hov, Ø., Brenquier, J.-L., Pandis, S. N., Facchini, M. C., Hansson, H.-C., Wiedensohler, A., and O'Dowd, C. D.: Introduction: European Integrated Project on Aerosol Cloud Climate and Air

- 5 Kulmala, M., Asmi, A., Lappalainen, H. K., Baltensperger, U., Brenguier, J.-L., Facchini, M. C.,  
Hansson, H.-C., Hov, Ø., O'Dowd, C. D., Pöschl, U., Wiedensohler, A., Boers, R., Boucher,  
O., de Leeuw, G., Denier van der Gon, H. A. C., Feichter, J., Krejci, R., Laj, P., Lihavainen,  
H., Lohmann, U., McFiggans, G., Mentel, T., Pilinis, C., Riipinen, I., Schulz, M., Stohl, A.,  
Swietlicki, E., Vignati, E., Alves, C., Amann, M., Ammann, M., Arabas, S., Artaxo, P., Baars,  
H., Beddows, D. C. S., Bergström, R., Beukes, J. P., Bilde, M., Burkhardt, J. F., Canonaco, F.,  
Clegg, S. L., Coe, H., Crumeyrolle, S., D'Anna, B., Decesari, S., Gilardoni, S., Fischer, M.,  
Fjaeraa, A. M., Fountoukis, C., George, C., Gomes, L., Halloran, P., Hamburger, T., Harrison,  
R. M., Herrmann, H., Hoffmann, T., Hoose, C., Hu, M., Hyvärinen, A., Hörrak, U., Iinuma, Y.,  
Iversen, T., Josipovic, M., Kanakidou, M., Kiendler-Scharr, A., Kirkevåg, A., Kiss, G., Klimont,  
Z., Kolmonen, P., Komppula, M., Kristjánsson, J.-E., Laakso, L., Laaksonen, A., Labonnote,  
L., Lanz, V. A., Lehtinen, K. E. J., Rizzo, L. V., Makkonen, R., Manninen, H. E., McMeeking,  
G., Merikanto, J., Minikin, A., Mirme, S., Morgan, W. T., Nemitz, E., O'Donnell, D., Panwar,  
T. S., Pawlowska, H., Petzold, A., Pienaar, J. J., Pio, C., Plass-Duelmer, C., Prévôt, A. S. H.,  
Pryor, S., Reddington, C. L., Roberts, G., Rosenfeld, D., Schwarz, J., Seland, Ø., Sellegrí,  
K., Shen, X. J., Shiraiwa, M., Siebert, H., Sierau, B., Simpson, D., Sun, J. Y., Topping, D.,  
Tunved, P., Vaattovaara, P., Vakkari, V., Veefkind, J. P., Visschedijk, A., Vuollekoski, H., Vuolo,  
R., Wehner, B., Wildt, J., Woodward, S., Worsnop, D. R., van Zadelhoff, G.-J., Zardini, A.  
A., Zhang, K., van Zyl, P. G., Kerminen, V.-M., S Carslaw, K., and Pandis, S. N.: General  
overview: European Integrated project on Aerosol Cloud Climate and Air Quality interactions  
(EUCAARI) – integrating aerosol research from nano to global scales, Atmos. Chem. Phys.,  
11, 13061–13143, doi:10.5194/acp-11-13061-2011, 2011.
- 25 Lesins, G., Chylek, P., and Lohmann, U.: A study of internal and external mixing scenarios and  
its effect on aerosol optical properties and direct radiative forcing, J. Geophys. Res., 107,  
doi:10.1029/2001JD000973, 2002.
- Lohmann, U. and Feichter, J.: Global indirect aerosol effects: a review, Atmos. Chem. Phys., 5,  
715–737, doi:10.5194/acp-5-715-2005, 2005.
- 30 Marcolli, C. and Krieger, U. K.: Phase changes during hygroscopic cycles of mixed or-  
ganic/inorganic model systems of tropospheric aerosols, J. Phys. Chem. A., 110, 1881–  
1893, doi:10.1021/jp0556759, 2006.

Estimation of  
aerosol composition  
from AERONET

A. J. van Beelen et al.

Title Page

Abstract

Introduction

Conclusions

References

Tables

Figures

◀

▶

◀

▶

Back

Close

Full Screen / Esc

Printer-friendly Version

Interactive Discussion



Estimation of aerosol composition from AERONET

A. J. van Beelen et al.

Title Page

Abstract

Introduction

Conclusions

References

Tables

Figures

◀

▶

◀

▶

Back Close

Full Screen / Esc

Printer-friendly Version

Interactive Discussion



McConnell, C. L., Formenti, P., Highwood, E. J., and Harrison, M. A. J.: Using aircraft measurements to determine the refractive index of Saharan dust during the DODO Experiments, *Atmos. Chem. Phys.*, 10, 3081–3098, doi:10.5194/acp-10-3081-2010, 2010.

Mensah, A. A., Holzinger, R., Otjes, R., Trimborn, A., Mentel, Th. F., ten Brink, H., Henzing, B., and Kiendler-Scharr, A.: Aerosol chemical composition at Cabauw, The Netherlands as observed in two intensive periods in May 2008 and March 2009, *Atmos. Chem. Phys.*, 12, 4723–4742, doi:10.5194/acp-12-4723-2012, 2012.

Meyer, N. K., Duplissy, J., Gysel, M., Metzger, A., Dommen, J., Weingartner, E., Alfarra, M. R., Prevot, A. S. H., Fletcher, C., Good, N., McFiggans, G., Jonsson, Å. M., Hallquist, M., Baltensperger, U., and Ristovski, Z. D.: Analysis of the hygroscopic and volatile properties of ammonium sulphate seeded and unseeded SOA particles, *Atmos. Chem. Phys.*, 9, 721–732, doi:10.5194/acp-9-721-2009, 2009.

Moelwyn-Hughes, E. A.: Physical Chemistry, 2nd rev. ed., p.397, Pergamon, New York, 1961.

Morgan, W. T., Allan, J. D., Bower, K. N., Esselborn, M., Harris, B., Henzing, J. S., Highwood, E. J., Kiendler-Scharr, A., McMeeking, G. R., Mensah, A. A., Northway, M. J., Osborne, S., Williams, P. I., Krejci, R., and Coe, H.: Enhancement of the aerosol direct radiative effect by semi-volatile aerosol components: airborne measurements in North-Western Europe, *Atmos. Chem. Phys.*, 10, 8151–8171, doi:10.5194/acp-10-8151-2010, 2010.

Nelder, J. A. and Mead, R.: A simplex method for function minimization, *The Computer Journal*, 7, 308–313, doi:10.1093/comjnl/7.4.308, 1965.

Oshima, N., Koike, M., Zhang, Y., and Kondo, Y.: Aging of black carbon in outflow from anthropogenic sources using a mixing state resolved model: 2. Aerosol optical properties and cloud condensation nuclei activities, *J. Geophys. Res.*, 114, D18202, doi:10.1029/2008JD011681, 2009.

Péré, J. C., Mallet, M., Bessagnet, B., and Pont, V.: Evidence of the aerosol core-shell mixing state over Europe during the heat wave of summer 2003 by using CHIMERE simulations and AERONET inversions, *Geophys. Res. Lett.*, 36, L09807, doi:10.1029/2009GL037334, 2009.

Petzold, A. and Schönlinner, M.: Multi-angle absorption photometry – a new method for the measurement of aerosol light absorption and atmospheric black carbon, *J. Aerosol Sci.*, 35, 421–441, 2004.

Petzold, A., Schloesser, H., Sheridan, P. J., Arnott, W. P., Ogren, J. A., and Virkkula, A.: Evaluation of multiangle absorption photometry for measuring aerosol light absorption, *Aerosol Sci. Technol.*, 39, 40–51, 2005.

## Estimation of aerosol composition from AERONET

A. J. van Beelen et al.

[Title Page](#)

[Abstract](#)

[Introduction](#)

[Conclusions](#)

[References](#)

[Tables](#)

[Figures](#)

◀

▶

[Back](#)

[Close](#)

[Full Screen / Esc](#)

[Printer-friendly Version](#)

[Interactive Discussion](#)



Quaas, J., Boucher, O., Bellouin, N., and Kinne, S.: Satellite-based estimate of the direct and indirect aerosol climate forcing, *J. Geophys. Res.*, 113, D05204, doi:10.1029/2007JD008962, 2008.

Quaas, J., Ming, Y., Menon, S., Takemura, T., Wang, M., Penner, J. E., Gettelman, A., Lohmann, U., Bellouin, N., Boucher, O., Sayer, A. M., Thomas, G. E., McComiskey, A., Feingold, G., Hoose, C., Kristjánsson, J. E., Liu, X., Balkanski, Y., Donner, L. J., Ginoux, P. A., Stier, P., Grandey, B., Feichter, J., Sednev, I., Bauer, S. E., Koch, D., Grainger, R. G., Kirkevåg, A., Iversen, T., Seland, Ø., Easter, R., Ghan, S. J., Rasch, P. J., Morrison, H., Lamarque, J.-F., Iacono, M. J., Kinne, S., and Schulz, M.: Aerosol indirect effects – general circulation model intercomparison and evaluation with satellite data, *Atmos. Chem. Phys.*, 9, 8697–8717, doi:10.5194/acp-9-8697-2009, 2009.

Richardson, C. B. and Hightower, R. L.: Evaporation of ammonium nitrate particles, *Atmos. Environ.*, 21, 971–975, 1987.

Roelofs, G.-J. and Kamphuis, V.: Cloud processing, cloud evaporation and Angström exponent, *Atmos. Chem. Phys.*, 9, 71–80, doi:10.5194/acp-9-71-2009, 2009.

Roelofs, G.-J., ten Brink, H., Kiendler-Scharr, A., de Leeuw, G., Mensah, A., Minikin, A., and Otjes, R.: Evaluation of simulated aerosol properties with the aerosol-climate model ECHAM5-HAM using observations from the IMPACT field campaign, *Atmos. Chem. Phys.*, 10, 7709–7722, doi:10.5194/acp-10-7709-2010, 2010.

Russchenberg, H. W. J., Bosveld, F., Swart, D. P. J., ten Brink, H., de Leeuw, G., Uijlenhoet, R., Arbesser-Rastburg, B., van der Marel, H., Ligthart, L., Boers, R., and Apituley, A.: Ground-based atmospheric remote sensing in The Netherlands; European outlook, *IEICE Transactions on Communications*, E88-B(6), 2252–2258, doi:10.1093/ietcom/e88-b.6.2252, 2005.

Russell, P. B., Bergstrom, R. W., Shinozuka, Y., Clarke, A. D., DeCarlo, P. F., Jimenez, J. L., Livingston, J. M., Redemann, J., Dubovik, O., and Strawa, A.: Absorption Angstrom Exponent in AERONET and related data as an indicator of aerosol composition, *Atmos. Chem. Phys.*, 10, 1155–1169, doi:10.5194/acp-10-1155-2010, 2010.

Schaap, M., Apituley, A., Timmermans, R. M. A., Koelemeijer, R. B. A., and de Leeuw, G.: Exploring the relation between aerosol optical depth and PM<sub>2.5</sub> at Cabauw, the Netherlands, *Atmos. Chem. Phys.*, 9, 909–925, doi:10.5194/acp-9-909-2009, 2009.

Schaap, M., Otjes, R. P., and Weijers, E. P.: Illustrating the benefit of using hourly monitoring data on secondary inorganic aerosol and its precursors for model evaluation, *Atmos. Chem. Phys.*, 11, 11041–11053, doi:10.5194/acp-11-11041-2011, 2011.

**Estimation of aerosol composition from AERONET**

A. J. van Beelen et al.

[Title Page](#)[Abstract](#)[Introduction](#)[Conclusions](#)[References](#)[Tables](#)[Figures](#)[|◀](#)[▶|](#)[Back](#)[Close](#)[Full Screen / Esc](#)[Printer-friendly Version](#)[Interactive Discussion](#)

Estimation of aerosol composition from AERONET

A. J. van Beelen et al.

Title Page

Abstract

Introduction

Conclusions

References

Tables

Figures

◀

▶

Back

Close

Full Screen / Esc

Printer-friendly Version

Interactive Discussion



- Svenningsson, B., Rissler, J., Swietlicki, E., Mircea, M., Bilde, M., Facchini, M. C., Decesari, S., Fuzzi, S., Zhou, J., Mønster, J., and Rosenørn, T.: Hygroscopic growth and critical supersaturations for mixed aerosol particles of inorganic and organic compounds of atmospheric relevance, *Atmos. Chem. Phys.*, 6, 1937–1952, doi:10.5194/acp-6-1937-2006, 2006.
- 5 Tang, I. N.: Chemical and size effects of hygroscopic aerosols on light scattering coefficients, *J. Geophys. Res.*, 101, 19245–19250, doi:10.1029/96JD03003, 1996.
- Tang, I. N.: Thermodynamic and optical properties of mixed-salt aerosols of atmospheric importance, *J. Geophys. Res.*, 102, 1883–1893, 1997.
- 10 Tang, I. N. and Munkelwitz, H. R.: Composition and temperature dependence of the deliquescence properties of hygroscopic aerosol, *Atmos. Environ.*, 27A, 467–473, doi:10.1016/0960-1686(93)90204-C, 1993.
- Tang, I. N. and Munkelwitz, H. R.: Water activities, densities, and refractive indices of aqueous sulfates and sodium nitrate droplets of atmospheric importance, *J. Geophys. Res.*, 20, 18801–18808, 1994.
- 15 Tang, I. N., Tridico, A. C., and Fung, K. H. Fung: Thermodynamic and optical properties of sea salt aerosols, *J. Geophys. Res.*, 102, 23269–23276, 1997.
- Tanré, D., Bréon, F. M., Deuzé, J. L., Dubovik, O., Ducos, F., François, P., Goloub, P., Herman, M., Lifermann, A., and Waquet, F.: Remote sensing of aerosols by using polarized, directional and spectral measurements within the A-Train: the PARASOL mission, *Atmos. Meas. Tech.*, 4, 1383–1395, doi:10.5194/amt-4-1383-2011, 2011.
- 20 ten Brink, H., Otjes, R., Jongejan, P., and Slanina, S.: An instrument for semi-continuous monitoring of the size-distribution of nitrate, ammonium, sulphate and chloride in aerosol, *Atmos. Environ.*, 41, 2768–2779, doi:10.1016/j.atmosenv.2006.11.041, 2007.
- Thomas, R. M., Trebs, I., Otjes, R., Jongejan, P. A. C., ten Brink, H., Phillips, G., Kortner, M., Meixner, F. X., and Nemitz, E.: An automated analyzer to measure surface-atmosphere exchange fluxes of water soluble inorganic aerosol compounds and reactive trace gases, *Environ. Sci. Technol.*, 43, 1412–1418, doi:10.1021/es8019403, 2009.
- 25 Toon, O. B., Pollack, J. B., and Khare, B. N.: Optical constants of several atmospheric aerosol species: ammonium sulfate, aluminum oxide, and sodium chloride, *J. Geophys. Res.*, 81, 5733–5748, doi:10.1029/JC081i033p05733, 1976.
- 30 Turpin, B. J. and Lim, H. J.: Species contributions to PM<sub>2.5</sub> mass concentrations: Revisiting common assumptions for estimating organic mass, *Aerosol Sci. Technol.* 35, 602–610, 2001.

**Estimation of aerosol composition from AERONET**

A. J. van Beelen et al.

- van Beelen, A. J. and van Delden, A. J.: Cleaner air brings better views, more sunshine and warmer summer days in the Netherlands, *Weather*, 67, 21–25, doi:10.1002/wea.854, 2012.
- Wagner, F., Bortoli, D., Pereira, S., Costa, M., Silva, A. M., Weinzierl, B., Esselborn, M., Petzold, A., Rasp, K., Heinold, B., and Tegen, I.: Properties of dust aerosol particles transported to Portugal from the Sahara desert, *Tellus B*, 61, 297–306, 2009.
- 5 Wagner, R., Ajtai, T., Kandler, K., Lieke, K., Linke, C., Müller, T., Schnaiter, M., and Vragel, M.: Complex refractive indices of Saharan dust samples at visible and near UV wavelengths: a laboratory study, *Atmos. Chem. Phys.*, 12, 2491–2512, doi:10.5194/acp-12-2491-2012, 2012.
- 10 Wang, J., Hoffmann, A. A., Park, R. J., Jacob, D. J., and Martin, S. T.: Global distribution of solid and aqueous sulfate aerosols: Effect of the hysteresis of particle phase transition, *J. Geophys. Res.*, 103, D11206, doi:10.1029/2007JD009367, 2008.
- Wang, K., Dickinson, R. E., and Liang, S.: Clear sky visibility has decreased over land globally from 1973 to 2007, *Science*, 323, 1468–1470, 2009.
- 15 Weast, R. C.: *Handbook of Chemistry and Physics*, 66th edn., CRC Press, Florida, USA, 1985.
- Weast, R. C.: *Physical constants of organic compounds*, CRC Handbook of Chemistry and Physics, 68th Edition, edited by: Weast, R. C., CRC Press, Boca Raton, FL, B67-B146, 1987.
- 20 Yu, H., Quinn, P. K., Feingold, G., Remer, L. A., Kahn, R. A., Chin, M., and Schwartz, S. E.: Remote Sensing and In Situ Measurements of Aerosol Properties, Burdens, and Radiative Forcing, in *Atmospheric Aerosol Properties and Climate Impacts*, A Report by the U.S. Climate Change Science Program and the Subcommittee on Global Change Research, edited by: Chin, M., Kahn, R. A., and Schwartz, S. E., National Aeronautics and Space Administration, Washington, DC, USA, 2009.
- 25 Zdanovskii, A. B.: Trudy Solyanoi Laboratorii Akad. Nauk SSSR, No. 2, 1936.
- Zieger, P., Weingartner, E., Henzing, J., Moerman, M., de Leeuw, G., Mikkilä, J., Ehn, M., Petäjä, T., Clémer, K., van Roozendael, M., Yilmaz, S., Frieß, U., Irie, H., Wagner, T., Shaiganfar, R., Beirle, S., Apituley, A., Wilson, K., and Baltensperger, U.: Comparison of ambient aerosol extinction coefficients obtained from in-situ, MAX-DOAS and LIDAR measurements at Cabauw, *Atmos. Chem. Phys.*, 11, 2603–2624, doi:10.5194/acp-11-2603-2011, 2011.
- 30

[Title Page](#)[Abstract](#)[Introduction](#)[Conclusions](#)[References](#)[Tables](#)[Figures](#)[◀](#)[▶](#)[◀](#)[▶](#)[Back](#)[Close](#)[Full Screen / Esc](#)[Printer-friendly Version](#)[Interactive Discussion](#)

## Estimation of aerosol composition from AERONET

A. J. van Beelen et al.

$x$	Description	Remarks
$m_f, m_c$ (so4)	column average mass mixing ratio sulfate	The inorganic composition is determined from sulfate by using (fixed) ammonium-to-sulfate and nitrate-to-sulfate ratios (see text).
$m_f, m_c$ (oc)	mass mixing ratio organic carbon	Water uptake is determined assuming 20 % wt levoglucosan, 40 % wt succinic acid and 40 % wt Suwannee river reference fulvic acid (Svenningsson et al., 2006).
$m_f, m_c$ (bc)	mass mixing ratio black carbon	–
$N_f, N_c$	column average number concentration	–
$\sigma_f, \sigma_c$	(geometric) standard deviation	Fine and coarse mode aerosols are lognormally distributed in 100 bins between 0.005 and 50 $\mu\text{m}$
RH	column average relative humidity	Initial guess is derived from sounding data.



## Estimation of aerosol composition from AERONET

A. J. van Beelen et al.

**Table 2.** Overview of the parameters in the measurement vector ( $\mathbf{y}$ ) and the uncertainties  $e_y$  in  $\mathbf{y}$ .

$y$	Description	$e_y$
RRI( $\lambda$ )	real part of the refractive index for 4 wavelengths ( $\lambda = 440, 675, 870, 1020\text{ nm}$ )	$E_{\text{RRI}} = \max [0.005\text{RRI}/\text{AOT}_{440\text{ nm}}, 0.025]$
IRI( $\lambda$ )	imaginary part of the refractive index	$E_{\text{IRI}} = \text{IRI} \max [1/(1 + 2.5(\text{AOT}_{440\text{ nm}} - 0.05)), 0.5]$
AOT( $\lambda$ )	aerosol optical thickness	$E_{\text{AOT}} = 0.02$
SSA( $\lambda$ )	single scattering albedo	$E_{\text{SSA}} = 0.07/(1 + 3(\text{AOT}_{440\text{ nm}} - 0.05))$
$V_i$	volume distribution in 22 bins	$E_V = 0.15V_i^*$
RH <sub>prior</sub>	column average relative humidity from soundings	$\sim 10\%^*$

\* Approximation, see text.

- [Title Page](#)
- [Abstract](#) | [Introduction](#)
- [Conclusions](#) | [References](#)
- [Tables](#) | [Figures](#)
- [◀](#) | [▶](#)
- [◀](#) | [▶](#)
- [Back](#) | [Close](#)
- [Full Screen / Esc](#)
- [Printer-friendly Version](#)
- [Interactive Discussion](#)



<a href="#">Title Page</a>	
<a href="#">Abstract</a>	<a href="#">Introduction</a>
<a href="#">Conclusions</a>	<a href="#">References</a>
<a href="#">Tables</a>	<a href="#">Figures</a>
<a href="#">◀</a>	<a href="#">▶</a>
<a href="#">◀</a>	<a href="#">▶</a>
<a href="#">Back</a>	<a href="#">Close</a>
<a href="#">Full Screen / Esc</a>	
<a href="#">Printer-friendly Version</a>	
<a href="#">Interactive Discussion</a>	

**Table 3.** Specific densities for the aerosol chemical components.

Compound	Dry density	Range	Reference
$(\text{NH}_4)_2\text{SO}_4$	1.76	–	1
$\text{NH}_4\text{HSO}_4$	1.78	–	1
$\text{H}_2\text{SO}_4$	1.841	–	2
NaCl	2.165	–	3, 4
Organic Matter	1.547*	1.2–1.8 (7, 8, 9, 10, 11)	1, 5
Black Carbon	1.8	1.0–2.0 (11, 12, 13)	12
Dust	2.65	2.5–2.75 (14, 15)	14
Water	0.9971	–	16

\* Weighted density from 20 % wt levoglucosan, 40 % wt succinic acid, and 40 % Suwannee river reference fulvic acid (Svenningsson et al., 2006). <sup>1</sup> Tang (1996), <sup>2</sup> Weast (1985), <sup>3</sup> Köpke et al. (1997), <sup>4</sup> Hess et al. (1998), <sup>5</sup> Weast (1985), <sup>6</sup> Svenningsson et al. (2006), <sup>7</sup> Turpin and Lim (2001), <sup>8</sup> Dick et al. (2000), <sup>9</sup> Hallquist et al. (2009), <sup>10</sup> Dinar et al. (2006), <sup>11</sup> Ganguly et al. (2009), <sup>12</sup> Bond and Bergstrom (2006), <sup>13</sup> Stelson (1990), <sup>14</sup> McConnell (2009), <sup>15</sup> Wagner et al. (2009) and references therein, <sup>16</sup> Tang and Munkelwitz (1994).



**Table 4.** Refractive indices for four different wavelengths (440, 675, 870 and 1020 nm) presented with a range found in the literature. When no imaginary part (*italic i*) is listed, it is assumed to be zero.

Compound	440 nm	675 nm	870 nm	1020 nm	Range	Reference
$(\text{NH}_4)_2\text{SO}_4$	1.535	1.525	1.52	1.52	–	1
$\text{NH}_4\text{HSO}_4$	1.48	1.47	1.465	1.465	–	2
$\text{H}_2\text{SO}_4$ (97% wt)	1.43	1.42	1.415	1.41	1.41–1.43 (2, 3, 4)	3
$\text{NaCl}$	1.56	1.546	1.534	1.532	1.49–1.55 (5, 6, 1)	1
$\text{NH}_4\text{NO}_3$	1.56	1.545	1.54	1.535	1.41–1.60 (7, 8, 9, 10)	6
Organics	$1.57 \text{ -}1.5e\text{-}2 i$	$1.55 \text{ -}5e\text{-}3 i$	$1.54 \text{ -}3e\text{-}3 i$	$1.535 \text{ -}3e\text{-}3 i$	$1.43\text{ -}1.65 2e\text{-}3 \text{ -}0.1 i$ (11, 12, 13)	13
Black carbon	$1.85 \text{ -}0.71 i$	$1.85 \text{ -}0.71 i$	$1.85 \text{ -}0.71 i$	$1.85 \text{ -}0.71 i$	$1.50\text{ -}2.0 0.44\text{ -}1.0 i$ (14, 16, 17, 18, 19)	15
Dust	$1.54 \text{ -}8e\text{-}3 i$	$1.52 \text{ -}5e\text{-}3 i$	$1.51 \text{ -}3e\text{-}3 i$	$1.51 \text{ -}3e\text{-}3 i$	$1.52\text{ -}1.58 1e\text{-}3 \text{ -}1e\text{-}2 i$ (20, 21, 22, 23)	20, 21
Water	1.344	1.331	1.324	1.321	–	24

<sup>1</sup> Toon et al. (1976), <sup>2</sup> Stelson (1990), <sup>3</sup> Benko et al. (2009), <sup>4</sup> Hess et al. (1998), <sup>5</sup> Shettle and Fenn (1979), <sup>6</sup> Tang (1996), <sup>7</sup> Weast (1987) from Benko et al. (2009) (550–589 nm), <sup>8</sup> Richardson and Hightower (1987) (633 nm), <sup>9</sup> Tang (1996), <sup>10</sup> Weast (1985), <sup>11</sup> Köpke et al. (1997), <sup>12</sup> Dinar et al. (2008), <sup>13</sup> Hoffer et al. (2006), <sup>14</sup> Horvath (1998), <sup>15</sup> Stier et al. (2007), <sup>16</sup> Bond and Bergstrom (2006), <sup>17</sup> Chang and Charalampopoulos (1990), <sup>18</sup> Janzen (1979), <sup>19</sup> Schuster et al. (2005), <sup>20</sup> Kinne et al. (2003), <sup>21</sup> Sokolik et al. (1993), <sup>22</sup> Wagner et al. (2012), <sup>23</sup> Kandler et al. (2011) (532 nm, Cape Verde), <sup>24</sup> Segelstein (1981).

- [Title Page](#)
- [Abstract](#) | [Introduction](#)
- [Conclusions](#) | [References](#)
- [Tables](#) | [Figures](#)
- [◀](#) | [▶](#)
- [◀](#) | [▶](#)
- [Back](#) | [Close](#)
- [Full Screen / Esc](#)
- [Printer-friendly Version](#)
- [Interactive Discussion](#)



**Estimation of aerosol composition from AERONET**

A. J. van Beelen et al.

**Table 5.** Correlations ( $R^2$ ) between model computed (optimized) values and AERONET inversions of the real and imaginary part of the refractive index (RRI and IRI), aerosol optical thickness (AOT), single scattering albedo (SSA) at four wavelengths, and relative humidity (RH) derived from radiosonde measurements for all data (including the “suspect” data) during the first 14 days of May.

Correlation ( $R^2$ )	440 nm	676 nm	870 nm	1020 nm
RRI	0.78	0.81	0.85	0.84
IRI	0.81	0.98	0.97	0.96
AOT	1.0	1.0	0.99	0.99
SSA	0.86	0.98	0.98	0.97
RH	0.98			

- [Title Page](#)
- [Abstract](#) | [Introduction](#)
- [Conclusions](#) | [References](#)
- [Tables](#) | [Figures](#)
- [◀](#) | [▶](#)
- [◀](#) | [▶](#)
- [Back](#) | [Close](#)
- [Full Screen / Esc](#)
- [Printer-friendly Version](#)
- [Interactive Discussion](#)



## Estimation of aerosol composition from AERONET

A. J. van Beelen et al.

**Table 6.** Mean (column-average) modeled ( $\mu_{\text{mod}}$ ) and mean observed ( $\mu_{\text{obs}}$ ) (near-surface) mass concentration ( $\mu\text{g m}^{-3}$ ) together with corresponding standard deviations ( $\sigma$ ) and modeled and observed medians ( $\text{med}_{\text{mod}}$  and  $\text{med}_{\text{obs}}$ ) during the first half of May 2008. Values including “suspect” data are presented between brackets.

Conc [ $\mu\text{g m}^{-3}$ ]	$\mu_{\text{mod}} \pm \sigma_{\text{mod}}$	$\mu_{\text{obs}} \pm \sigma_{\text{obs}}$	$\text{med}_{\text{mod}}$	$\text{med}_{\text{obs}}$
Total dry	$32.7 \pm 11.6$ ( $38.5 \pm 25.2$ )	$32.0 \pm 10.8$ ( $30.2 \pm 11.2$ )	29.2 (31.5)	30.3 (28.7)
BC	$0.70 \pm 0.29$ ( $0.75 \pm 0.34$ )	$0.94 \pm 0.36$ ( $0.97 \pm 0.43$ )	0.67 (0.71)	0.83 (0.91)
$\text{SO}_4$	$6.28 \pm 3.72$ ( $8.26 \pm 5.31$ )	$4.47 \pm 1.33$ ( $4.37 \pm 1.38$ )	5.70 (7.21)	4.87 (4.69)
$\text{NH}_4$	$4.59 \pm 2.72$ ( $6.03 \pm 3.88$ )	$3.43 \pm 1.55$ ( $3.35 \pm 1.57$ )	4.17 (5.27)	3.05 (3.23)
$\text{NO}_3$	$8.47 \pm 5.02$ ( $11.1 \pm 7.17$ )	$7.97 \pm 3.70$ ( $7.48 \pm 4.35$ )	7.70 (9.73)	7.71 (7.04)
OC	$12.7 \pm 7.84$ ( $12.3 \pm 21.9$ )	$15.0 \pm 5.16$ ( $13.9 \pm 5.37$ )	12.3 (8.72)	14.6 (14.1)

- [Title Page](#)
- [Abstract](#) | [Introduction](#)
- [Conclusions](#) | [References](#)
- [Tables](#) | [Figures](#)
- [◀](#) | [▶](#)
- [◀](#) | [▶](#)
- [Back](#) | [Close](#)
- [Full Screen / Esc](#)
- [Printer-friendly Version](#)
- [Interactive Discussion](#)



## Estimation of aerosol composition from AERONET

A. J. van Beelen et al.

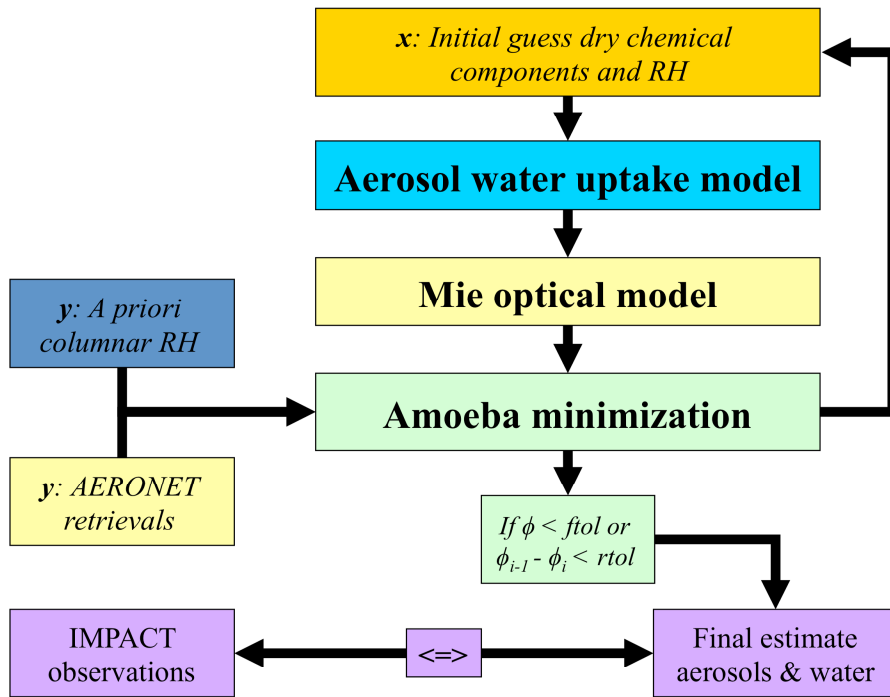


**Fig. 1.** Flow diagram of the model. The state vector  $x$  contains the initial guess, which can be updated by the minimization routine which compares the output of the model with the measurement vector  $y$ . When the cost function  $\phi$  has reached a value lower than a certain threshold  $ftol$ , or when the improvement of  $\phi$  in subsequent runs is smaller than  $rtol$  a final estimate of the aerosol is obtained and compared to observations.

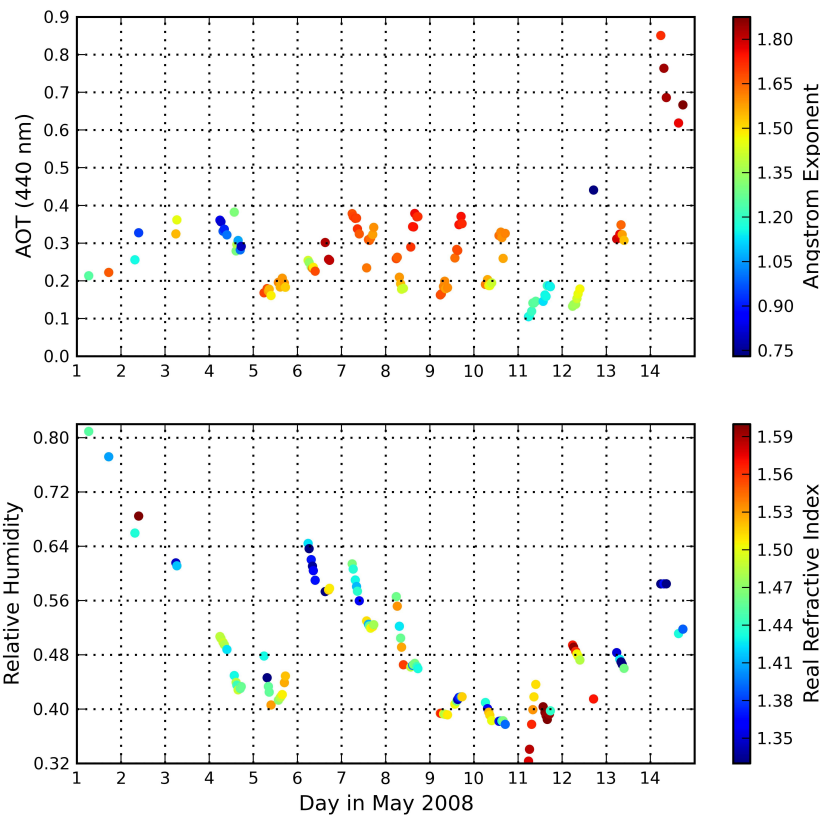


**Fig. 2.** AERONET level 1.5 inversion data during the first 14 days of May 2008 at the Cabauw Tower. Top panel: aerosol optical thickness (AOT) color coded with values of the Ångström exponent (440–675 nm). Bottom: The altitude weighted average relative humidity from balloon soundings between 0 and 2 km color coded with the AERONET real part of the refractive index.

**Estimation of aerosol composition from AERONET**

A. J. van Beelen et al.

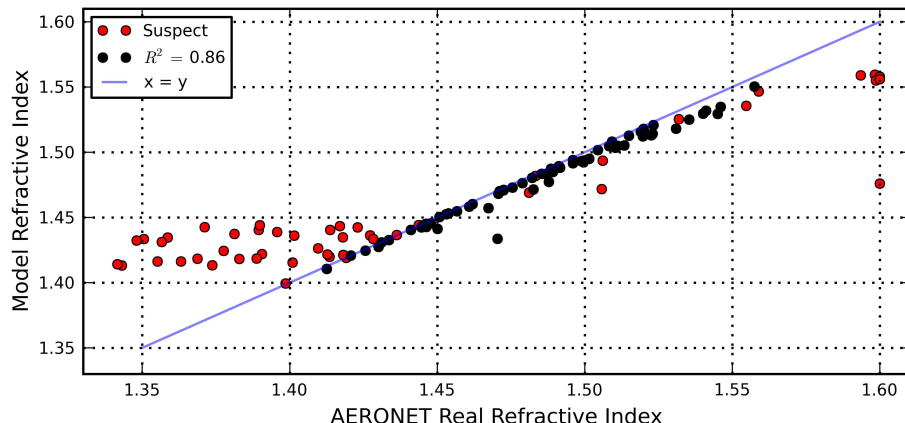


**Fig. 3.** Correlation between model computed (optimized) and AERONET real part of the refractive index, averaged over 4 wavelengths. Blue line shows the 1 : 1 ratio. Model results have been marked “suspect” (red) when the AERONET refractive index is outside the range that our model can simulate and/or when the cost function is larger than 10.

[Title Page](#)[Abstract](#)[Introduction](#)[Conclusions](#)[References](#)[Tables](#)[Figures](#)[|◀](#)[▶|](#)[Back](#)[Close](#)[Full Screen / Esc](#)[Printer-friendly Version](#)[Interactive Discussion](#)

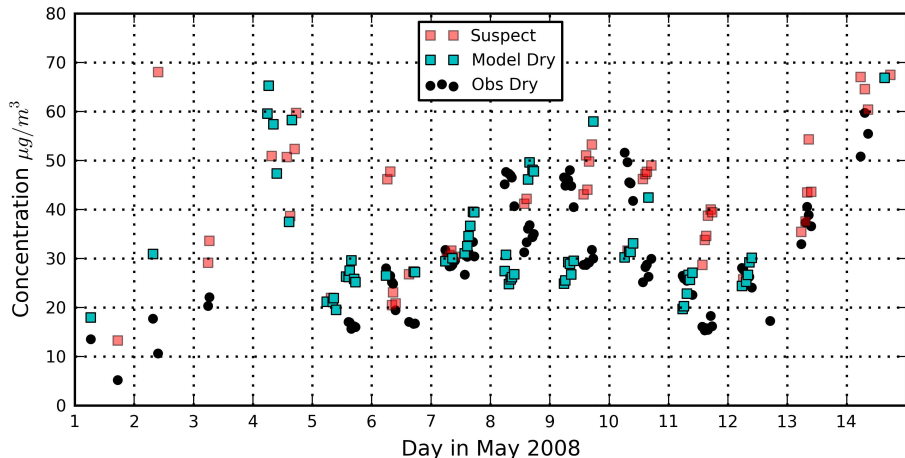


**Fig. 4.** Time series of total dry mass concentration from surface measurements (black dots), and our model results (cyan, red squares) during the first half of May 2008 at the Cabauw Tower.

Discussion Paper

Discussion Paper

Discussion Pap

Discussion Pa

Title Page

## Abstract

Introduction

### Conclusions

## References

Tables

## Figures

Books

Class

Full Screen / Esc

[Printer-friendly Version](#)

Interactive Discussion



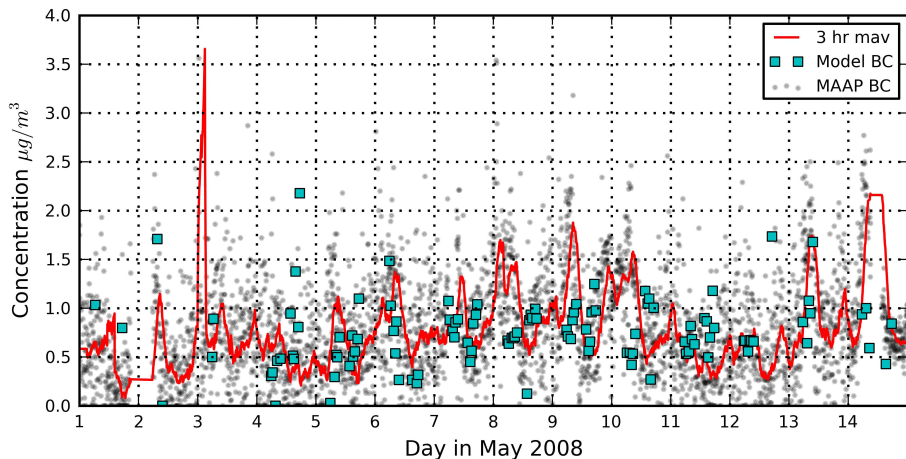


**Fig. 5.** Time series of black carbon concentration from surface observations (TNO multi-angle absorption photometer, black dots) with three hour centered moving average (red line), and our model results (cyan squares).

**Estimation of aerosol composition from AERONET**

A. J. van Beelen et al.

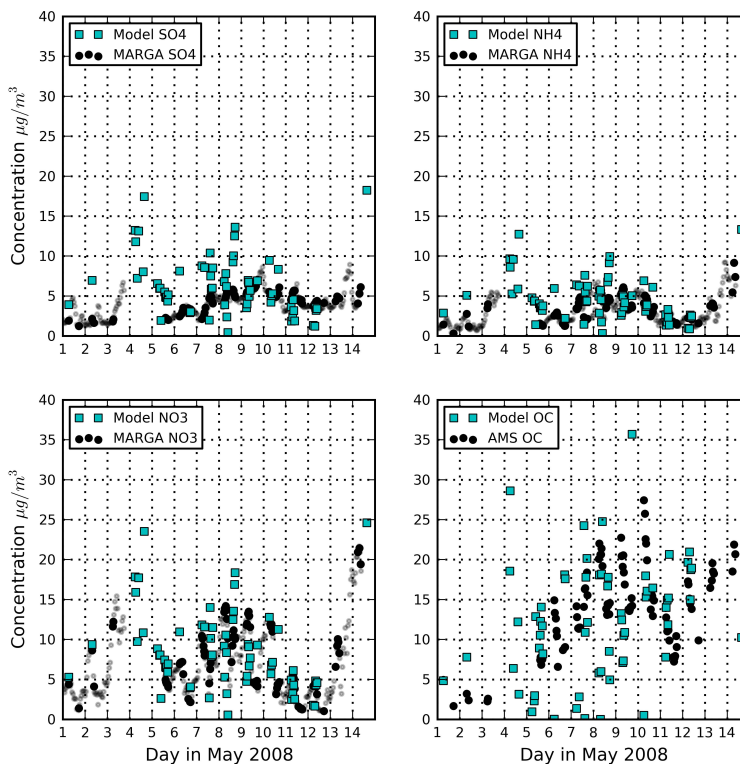


**Fig. 6.** Inorganic salt ion concentrations  $\text{SO}_4^{2-}$  (upper left),  $\text{NH}_4^+$  (upper right),  $\text{NO}_3^-$  (lower left) from surface observations of the MARGA (small grey dots), and organic matter from Jülich ICG-2 AMS (scaled to  $\text{PM}_{10}$ , lower right), interpolated to AERONET times (bold black dots) and compared to the column average model results (cyan squares). Values corresponding to suspect AERONET refractive indices have been left out.

**Estimation of aerosol composition from AERONET**

A. J. van Beelen et al.

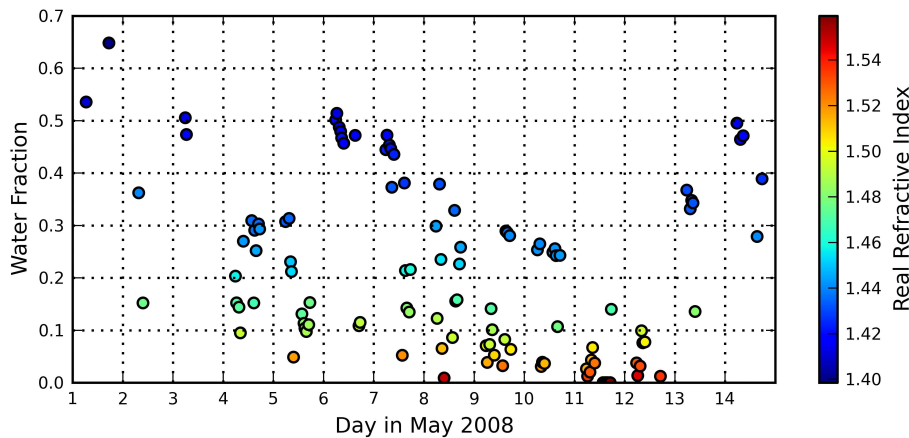


**Fig. 7.** Calculated water volume fraction, and optimized real refractive index (color filled).

- [Title Page](#)
- [Abstract](#) [Introduction](#)
- [Conclusions](#) [References](#)
- [Tables](#) [Figures](#)
- [◀](#) [▶](#)
- [◀](#) [▶](#)
- [Back](#) [Close](#)
- [Full Screen / Esc](#)
- [Printer-friendly Version](#)
- [Interactive Discussion](#)

**Estimation of aerosol composition from AERONET**

A. J. van Beelen et al.

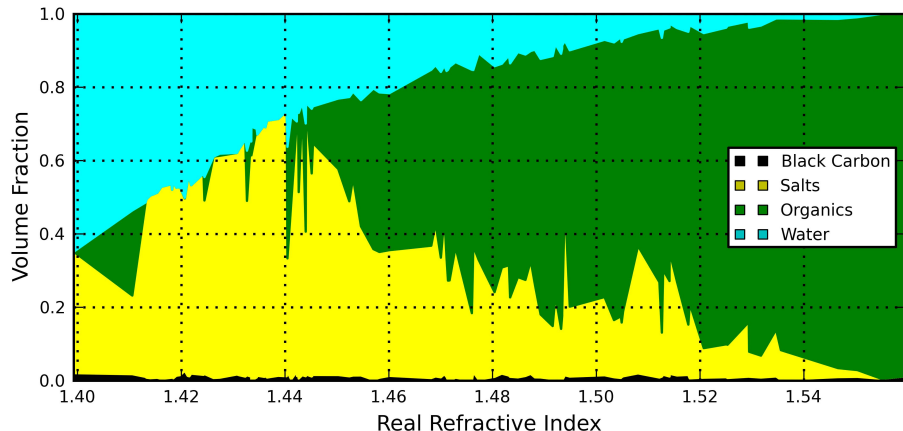


**Fig. 8.** Volume fraction of the modeled aerosol components as a function of the optimized real refractive index during May 2008. Here, the sum of (ammonium) sulfates and ammonium nitrate has been taken into “salts”, because their ratio is held constant throughout the retrieval.

[Title Page](#)  
[Abstract](#) [Introduction](#)  
[Conclusions](#) [References](#)  
[Tables](#) [Figures](#)

[◀](#) [▶](#)  
[◀](#) [▶](#)  
[Back](#) [Close](#)

[Full Screen / Esc](#)  
[Printer-friendly Version](#)  
[Interactive Discussion](#)

